JETIR.ORG ISSN: 2349-5162 | ESTD Year : 2014 | Monthly Issue
JOURNAL OF EMERGING TECHNOLOGIES AND INNOVATIVE RESEARCH (JETIR)
An International Scholarly Open Access, Peer-reviewed, Refereed Journal

ACTIVE REACTIVE POWER CONTROL OF A DOUBLY FED INDUCTION GENERATOR USING FPGA BASED WIND ENERGY CONVERSION SYSTEM

[1]AKHILA PORIKA [2]DR G SURESH BABU

[1]PG Scholar, Department of EEE, Chaitanya Bharathi Institute of Technology Gandipet, Hyderabad
[2]Professor, Department of EEE, Chaitanya Bharathi Institute of Technology Gandipet, Hyderabad

***Abstract*:** Wind power production is one of the most alluring renewable energy sources because of its widespread availability and the economic advantages of producing electricity on a massive scale. As a result, there is an ever-increasing reliance on massive wind turbines and wind farms as a source of renewable energy. DFIG's benefits in decoupled active and reactive power management are driving its increasing adoption in wind farms. However, DFIG is very vulnerable to grid failures, which is a major drawback. The active and reactive power of the DFIG must be regulated for it to function well. Overheating components due to reactive power may drastically reduce their useful lifespan. Power factor regulation is another service that may be provided by DFIG via management of the reactive power exchange with the grid. The amount of torque imparted to the rotor shaft directly correlates to the amount of active and reactive power generated. The magnitude of the rotor excitation voltage determines the amount of reactive power produced. Deep nuclei and red nuclei go via the brain stem to link the cerebellum and the cerebral cortex, where they deliver an action signal. The Multi Modular Joint-Brain controller (MMJ-BC) is a computational model generated by inspirational linkages. Nonlinear dynamical systems, such the position control of the Doubly Fed Induction Generator (DFIG), are used to verify the efficacy of the proposed MMJ-BC controller. Comparisons to the current Cerebrum (BELBIC) and Cerebellum-based controllers are used to verify the acquired findings from the performance analysis of the MMJ-BC under different operating situations. From the simulation findings, we learn that a Field Programmable Gate Array (FPGA) is used to regulate both the active and reactive powers by modifying the speed and the rotor excitation voltage, respectively.

IndexTerms: **Multi Modular Joint-Brain controller (MMJ-BC), Field Programmable Gate Array (FPGA), and Doubly Fed Induction Generator (DFIG) are some examples of index terms. Power, both proactive and reactive.**

I. INTRODUCTION

Rapid urbanisation and expanding industries are driving a relentless and alarming increase in the need for electricity. Due to the increasing need for energy, renewable power production from sources such as solar and wind has become more attractive in recent years. In terms of cost and dependability, modern wind power holds its own against more conventional energy options. There has been a recent surge in the construction of wind farms throughout the globe. Doubly-fed induction generators (DFIGs) are used in variable-speed wind generating systems. The wind's velocity fluctuates at irregular intervals. The active and reactive power flows from a wind generator like a DFIG must be controlled in a Wind Energy Conversion System (WECS). In a WECS, DFIGs are often favoured because of their cost-effective variable-speed operation. Direct Power Control (DPC) is a method reported in a number of scholarly works for independently regulating active and reactive power flow. A stator flux-oriented vector control system for active and reactive powers in a DFIG-based WECS is presented. Precision machine characteristics including moment of inertia, mutual inductance, stator resistance, and rotor resistance are needed for the controller design in traditional Vector Control (VC). When the WECS parameters are not accurately reflected, performance suffers. The energy output of DFIGs is higher, while their converter ratings are lower. The DFIG-based WECS is said to be controlled by a plethora of nonlinear controllers. Probability and Statistics Long calculation times are needed for controllers because of the optimisation work that goes into their design. An approach is developed to improve reactive power management and DC-link voltage control using vector control of direct current. When it comes to controlling the voltage source converters in WECS, the vast majority of published methods have considered proportional integral controllers or hysteresis-based controllers. An enhanced sliding mode controller is constructed with the help of shaft speed and aerodynamic torque, and the sliding surface is refined with the help of a nonlinear disturbance observer. There has been extensive research into the design of active and reactive power controllers for WECS, but a simple, reliable controller that is cost-effective and usable in real-time is still needed. Therefore, it is crucial to develop adaptive controllers that can still provide sufficient control performance even when the rotor speed or DFIG parameters vary. In this study, we design a WECS active and reactive power regulation system based on a sliding mode in a stator voltage-oriented frame.

The Reactive and Active Forces of the Stator Control

Method with a Focus on the Stator Field: Aligning the stator flux linkage with the direct axis of the PARK reference frame [22, 30] allows for independent regulation of the stator's active and reactive powers. While the stator flux vector is often employed for

DFIG control, additional alignment options such as the stator voltage vector and the rotor flux linkage may be found in the literature. By using this method, the rotor current vector may be broken down into its direct and quadrature components, the former of which is associated with reactive power and the latter with active power regulation.

By reducing the number of variables in the stator flux equations, the connection between the rotor and stator currents may be derived.

$$I_{sd} = \frac{\phi_{sd}}{L_s} - \frac{M}{L_s} I_{rd} \quad (1)$$

$$I_{sq} = -\frac{M}{L_s} I_{rq} \quad (2)$$

By substituting the foregoing equations into (8), the rotor flux may be represented in terms of rotor currents.

$$\phi_{rd} = \left(L_r - \frac{M^2}{L_s}\right) i_{rd} + \frac{M}{L_s}\phi_{sd} \quad (3)$$

$$\phi_{rq} = \left(L_r - \frac{M^2}{L_s}\right) i_{rq} \quad (4)$$

The rotor voltage dynamics in terms of rotor currents may be obtained by plugging the preceding equations into equation (7).

$$V_{rd} = R_r I_{rd} + \left(L_r - \frac{M^2}{L_s}\right)\frac{dI_{rd}}{dt} - \left(L_r - \frac{M^2}{L_s}\right)(\omega_s - \omega_m) I_{rq} + \frac{M}{L_s}\frac{d\phi_{sd}}{dt} \quad (5)$$

$$V_{rq} = R_r I_{rq} + \left(L_r - \frac{M^2}{L_s}\right)\frac{dI_{rq}}{dt} - \left(L_r - \frac{M^2}{L_s}\right)(\omega_s - \omega_m) I_{rd} + \frac{M}{L_s}(\omega_s - \omega_m)\phi_{sd} \quad (6)$$

Estimating the link between the rotor currents and the stator active and reactive powers is necessary for expressing the rotor voltages in terms of those powers. Because large-scale Wind turbines don't need to worry about the voltage drop in the stator resistance, we may simplify our formulations of stator powers to the following formulae.

$$P_s = -\frac{3}{2} V_s \frac{M}{L_s} I_{rq} \quad (7)$$

$$Q_s = \frac{3}{2}\frac{\phi_{sd}}{L_s} V_s - \frac{3}{2}\frac{M}{L_s} V_s I_{rd} \quad (8)$$

Finally, the stator active and reactive powers may be dynamically determined by rewriting the rotor voltage equations as follows:

Method based on adaptive sliding mode: In order to manage several types of nonlinear systems, the very effective method of adaptive sliding mode control (ASMC) was created. This control technique is chosen because it is easy to apply and yields a sufficient dynamical response [32], allowing it to be used in spite of external disruptions and modelling errors affecting the controlled process. The ASMC involves guiding a trajectory of a state variable towards stable surfaces and gliding over them until a balance point is reached. By adjusting the adaptive gain, the ASMC may function better. In order to guarantee stability and locate the ideal trajectory for the state variable, this value is derived using Lyapunov's theorem [33]. In this study, this method is utilised to determine the rotor voltage references necessary to maintain optimum active and reactive powers. There are three stages in the creation of these controllers:

Stability analysis

Calculation of control signals

Design of sliding surfaces

II. Analysis of Wind Generators

The mechanical shaft's behaviour may be described by the swing equation (13). Our primary interest is in the Maximum Power Point Tracking (MPPT) area (shown in Figure 3 as region 2 of the power-speed curve). The goal here is to harvest as much energy as possible from the wind when it is below the rated speed. The control of the wind turbine is discussed in terms of several tactics for following the Maximum Power Point curve. In this study, the electromagnetic torque, which is theoretically represented as a quadratic function of the turbine speed t, is regulated by means of an indirect speed controller. The appropriate degree of pitch is maintained here. Wind turbines in the MPPT zone have the coefficients shown in (14) [4] if the preceding argument holds.

It was shown that the DFIG electromagnetic torque is related to the turbine torque. The turbine and machine damping coefficients, Dt and Dm, respectively, and the gearbox ratio, N, are shown in this equation. If both damping coefficients are ignored, however, a simpler but less precise model is produced [4].

$$T_{em} = -\frac{T_t}{N} + (D_t + D_m)\omega_{rm} \quad (9)$$

$$= -k_{opt}\omega_{rm}^2 + (D_t + D_m)\omega_{rm} \quad (10)$$

$$k_{opt} = \frac{1}{2}\rho\pi\frac{R^5}{\lambda_{opt}^3 N^3} C_{p,max} \quad (11)$$

$$\omega_{rm} = N\Omega_t \quad (12)$$

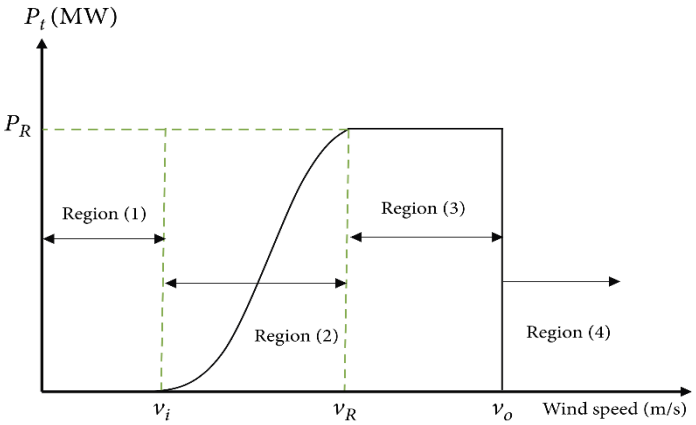

Figure1. Wind turbines' power vs wind speed graph.

III. Mathematical Models

Figure 2 depicts the standard setup for a DFIG that is linked to the grid, with the stator providing the grid with a constant voltage amplitude and frequency. A three-phase back-to-back converter, coupled to the rotor, may generate variable-amplitude and frequency three-phase voltages. By modulating the rotor's rotational velocity, a variety of operational states may be attained. This allows for precise regulation of the process, resulting in maximum power generation. When set at a constant speed, this function is disabled.

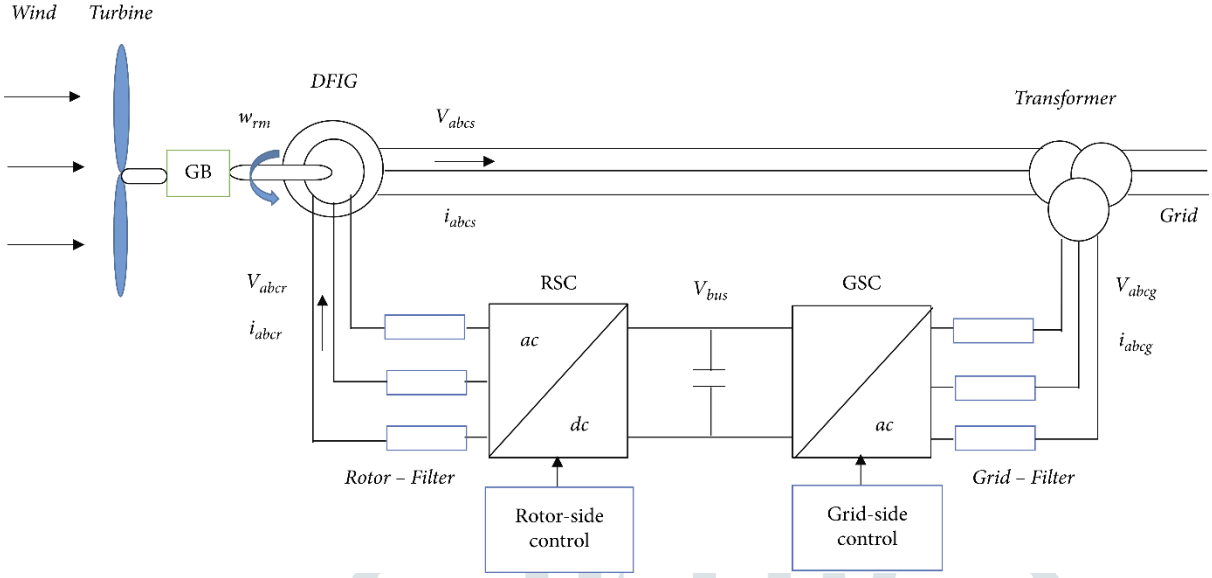

Figure2. A common setup for DFIGs based on wind turbines linked to the grid.

IV. DFIG Model

The mathematical model of the DFIG machine is most often represented by the dynamic (d-q) (synchronous) rotating reference frame. Relationships controlling the stator voltage (vds, vqs), the rotor voltage (vdr, vqr), the stator magnetic flux (ψds, ψqs), and the rotor magnetic flux (Ls=Lm+Lr) may be stated once the necessary rotational transformations are applied.

$$V_{ds} = R_s i_{ds} + \frac{d\Psi_{ds}}{dt} - \omega_s \Psi_{qs} \quad (13)$$

$$V_{qs} = R_s i_{qs} + \frac{d\Psi_{qs}}{dt} - \omega_s \Psi_{ds} \quad (14)$$

$$V_{dr} = R_r i_{dr} + \frac{d\Psi_{dr}}{dt} - \omega_r \Psi_{qr} \quad (15)$$

$$V_{qr} = R_r i_{qr} + \frac{d\Psi_{qr}}{dt} - \omega_s \Psi_{dr} \quad (16)$$

By rearranging the preceding model as shown by equations (15)-(16), we can extract the time derivative of the stator and rotor currents, where $\sigma = 1 - {L_m^2}/{L_r L_s}$

$$\frac{d}{dt} i_{ds} = \frac{1}{\sigma L_s}\left\{v_{ds} - R_s i_{ds} - \frac{L_m}{L_r} v_{dr} + \frac{L_m R_r}{L_r} i_{dr} + \left(\omega_s L_s - \frac{L_m^2 \omega_r}{L_r}\right) i_{qs} + (\omega_s - \omega_r) L_m i_{qr}\right\} \quad (17)$$

$$\frac{d}{dt} i_{qs} = \frac{1}{\sigma L_s}\left\{v_{qs} - R_s i_{qs} - \frac{L_m}{L_r} v_{qr} + \frac{L_m R_r}{L_r} i_{qr} + \left(\frac{L_m^2 \omega_r}{L_r} - \omega_s L_s\right) i_{ds} + (\omega_r - \omega_s) L_m i_{dr}\right\} \quad (18)$$

$$\frac{d}{dt} i_{dr} = \frac{1}{\sigma L_r}\left\{v_{dr} - R_r i_{dr} - \frac{L_m}{L_s} v_{ds} + \frac{L_m R_s}{L_s} i_{ds} + \left(\omega_r L_r - \frac{L_m^2 \omega_s}{L_s}\right) i_{qr} + (\omega_r - \omega_s) L_m i_{qs}\right\} \quad (19)$$

$$\frac{d}{dt} i_{qr} = \frac{1}{\sigma L_r}\left\{v_{qr} - R_r i_{qr} - \frac{L_m}{L_s} v_{qs} + \frac{L_m R_s}{L_s} i_{qs} + \left(\frac{L_m^2 \omega_s}{L_s} - \omega_r L_r\right) i_{dr} + (\omega_s - \omega_r) L_m i_{ds}\right\} \quad (20)$$

By comparing stator and rotor voltages and currents in the synchronous reference frame (21), reactive power may be determined. Evaluating the electromagnetic torque in the dq reference frame is also possible, as shown by (23) [2].

$$P_s = \frac{3}{2}\left(V_{ds} i_{ds} + v_{qs} i_{qs}\right) \quad (21)$$

$$P_r = \frac{3}{2}\left(V_{dr} i_{dr} + v_{qr} i_{qr}\right) \quad (22)$$

$$Q_s = \frac{3}{2}\left(V_{qs} i_{ds} + v_{ds} i_{qs}\right) \quad (23)$$

$$Q_r = \frac{3}{2}\left(V_{qr} i_{dr} + v_{dr} i_{qr}\right) \quad (24)$$

$$T_{em} = \frac{3PL_m}{4L_s}\left(\Psi_{qs} i_{dr} + \Psi_{ds} i_{qr}\right) \quad (25)$$

V. Modeling of Grid-Side System

A grid-side converter (GSC), filter, and grid voltages are all part of the grid-side system, which is seen in Figure 2. The amplitude and frequency of the grid voltages V_ga,V_gb,V_gcare constant while the system is in a steady state. At the same time, the amplitude and frequency of the output voltages V_fa,V_fb,V_fc may be adjusted. This analysis may be applied to the simplest possible grid filter setup, which consists of a pure inductive filter Lf and a parasitic resistance Rf. The (d-q) components of GSC voltages are expressed by transforming the electrical relationships shown in Figure 2. Therefore, the active power and reactive power of the grid in the d-q reference frame may be calculated as shown [4].

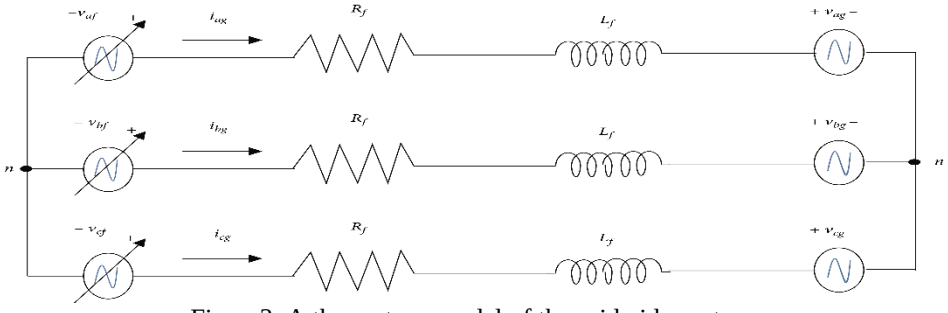

Figure3. A three-stage model of the grid-side system.

VI. Modeling of DC Link

Installed between the RSC and GSC, the DC link capacitor stores energy and has a capacitance of Cbus. The rotor's magnetising current is supplied by this reactive power source. If converter losses are disregarded, the DC bus power Pdc may be calculated as the output of the rotor less the input of the grid. The following equation [39] demonstrates a different way of expressing the DC link power necessary for monitoring the DC bus voltage.

$$P_{dc} = P_r - P_g = v_{dc} i_{dc} = v_{dc} C_{dc} \frac{dv_{dc}}{dt} \qquad (26)$$

VII. Grid Support for Real and Reactive Power

Newly installed technologies must be increasingly engaged in grid reliability elements under normal operating circumstances and during contingencies if renewable energy penetration is to increase. Active power manipulation is used in ancillary services to provide frequency control. However, voltage regulation is simplified by controlling reactive power at the point of common connection. Sometimes, wind farms must limit or spill available electricity due to congestion or inertia-related concerns. This subsection's stated goal is to assess the DFIG's wind turbine-based reactive power assistance capacity and actual power reductions.

A. Reactive Power Limits

There are numerous restrictions on how much reactive power assistance DFIG can provide. It is important to never exceed the rated currents of the stator or rotor. In addition, while supplying reactive power, the grid-side converter's (GSC) working restrictions must be respected [40].

In order to assess the reactive power constraints during MPPT operation, the steady-state model in the (d-q) reference frame may be utilised. As was already determined, iqr, the quadrature current of the rotor, is directly proportional to the real power of the stator. However, the rotor's direct current component idr is connected to the stator's reactive power. To accomplish the MPPT, iqr is fixed and cannot be changed. An analytical formula for iqr at any given wind speed is provided by (28) after iqr is extracted from equation (27) at steady state. Then, the largest idr component of the rotor current may be calculated. The maximum reactive power allowed by the stator is then determined by plugging in (idr-max).

$$i_{qr} = \frac{4k_{opt}\omega_{rm}^2 L_s}{3P\Psi_{ds}L_m} \qquad (27)$$

$$\omega_{rm} = \frac{\lambda_{opt}^3 v_\omega N}{R} \qquad (28)$$

and yet, the stator current limit as opposed to the rotor current limit can be the limiting factor for reactive power supply. The component of the quadrature current through the stator, denoted by the symbol iqs, is calculated after iqr is calculated for a given wind speed. Thus, the largest d-axis stator component may be determined. Therefore, the equation is used to determine the stator reactive power given a maximum stator current.

$$i_{qs} = -\frac{L_m}{L_s} i_{qr} \qquad (29)$$

The restrictions imposed by the rotor and stator currents gave rise to two distinct limits. However, whose limits are met first will decide the true reactive power capabilities. Furthermore, the maximum power point tracking (MPPT) restricts the amount of reactive power that may be taken in or sent out. Therefore, enabling active power curtailments may enhance reactive power assistance.

A. Real Power Curtailment

Active power ancillary services, such as frequency control and spinning reserves, are another area where wind turbines may contribute. In such instances, the process is not conforming to MPPT. As an alternative, partial curtailment is implemented to provide a genuine power buffer that may be used in times of crisis. Reducing active power consumption also boosts a machine's capacity to use reactive power. The MPPT area is reached and the pitch control mechanism is activated to accomplish the curtailment. One mechanical representation of the dynamic relationship between desired and actual pitch angles is called a "pitch actuator." In Figure 6, we can see a first-order model of a servomotor-driven pitch control system. The time derivative of the pitch angle may be characterised as (79), based on the estimated nonlinear dynamics of the pitch control system [44]. A new input * and state variable are included into this equation to describe the state-space model.

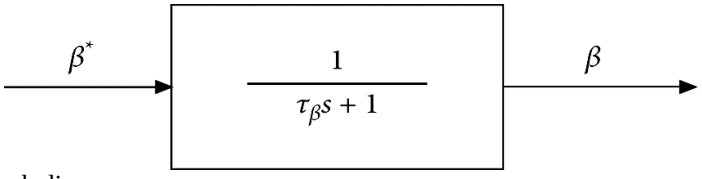

Figure4. Pitch control system block diagram.

$$\frac{d\beta}{dt} = \frac{1}{\tau_\beta}(\beta^* - \beta) \qquad (30)$$

Wind turbines should have a pitch angle and tip speed ratio that allows them to operate at their Maximum Power Point. Increasing the pitch angle decreases the power output by an amount proportionate to the power content of the predominant wind. This is done in order to get just the active power that is needed. The necessary output power is specified for a given wind speed, with a ceiling set by the most power that can be efficiently extracted. From this, we can calculate the power coefficient Cp that leads to the power savings shown by equation (1). The relationship between Cp and is seen in Figure 7 for a variety of pitch angles. It is necessary to choose and from these curves in order to get the predicted Cp that restricts the mechanical power of the turbine.

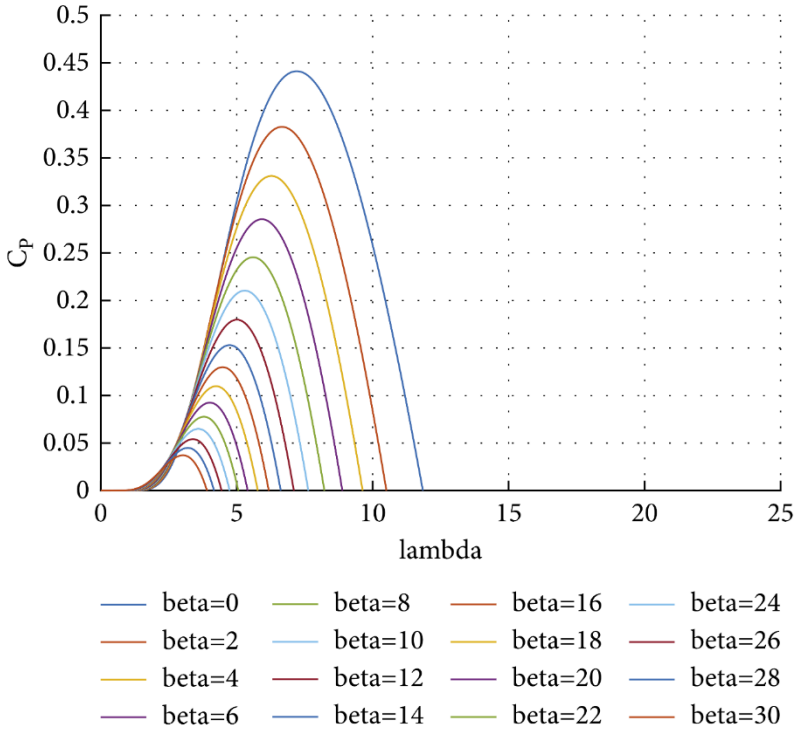

Figure5. For a range of pitch angles (with wind speed held constant at 8 m/s), we plot the relationship between the power coefficient and the tip speed ratio.

VIII. Controller

This paper's computational model is motivated by the neural connections between different regions of the brain, particularly the cerebellum's and the cerebrum's DN and RN. The phrase "Multi modular Joint-Brain Controller" (MMJ-BC) refers to the created controller-inspiring connections between the cerebellum and the cerebrum via the RN in the brainstem. Separate controllers for the cerebrum and cerebellum are established and then brought together with DN and RN in the design of MMJ-BC. The Cerebellum-based controller, known as BELBIC, takes its cues from the Limbic system and its accompanying components, whereas the brain's Cerebrum is responsible for the design of the cerebellum-based controller. MMJ-BC is built by sending Cerebellum data via DN for transmission to the RN, where it is analysed along with BELBIC data [19]. Testing on several plants, including the position control of an aircraft system and the speed control of a Brushless DC (BLDC) motor, validates the MMJ-BC's performance. We compare the suggested controller's performance to that of the traditional PID controller, as well as to that of the intelligent controllers BELBIC and Cerebellum.

A. Development of MMJ-BC

The brain is a mammalian mammal's most sensitive organ, processing sensory data from other parts of the body to make decisions [14, 15]. As can be seen in Fig. 1, the brain's exceedingly complex neuronal organisation is divided between the cerebrum, the cerebellum, and the brain stem.By studying the actions and processes involved in gathering information from various brain regions, the cognitive behaviour of mammals may be represented as a controller or algorithm. The brain's innate intelligence allows it to learn how to juggle several responsibilities. Intelligent controllers that take their cue from the structure and function of the mammalian brain are being developed [20]. The cerebrum is the biggest region of the brain, and its limbic system processes sensory inputs including language, taste, balance, hearing, and touch to generate emotional responses. The brain must respond quickly to these feelings by sending signals to the organ so that it can make a choice. The amygdala, orbitofrontal cortex (OFC), sensory cortex, thalamus, sensory signals, and emotional cue or reward signals are all components of the computational model for the limbic system. Different from the OFC, the amygdala serves as a quick and noisy output learning mechanism. The OFC learning system filters out unnecessary amygdala input and provides crucial motor cortex output. The Cerebellum, the region of the brain below the Cerebrum, is responsible for processing sensory input from the body's organs and the spinal cord. Posture, balance, coordination, and speech are all examples of voluntary motions controlled by the cerebellum, which is also critical for learning motor skills [21, 22]. Cerebellum Model Articulation Controller (CMAC) is a computer model for the Cerebellum consisting of mossy fibre, Granule cell, Parallel Fibre, Climbing Fibre, and Purkinjie Cell [18]. In order to make the best possible judgements for the work at hand, the Climbing Fibre (CF) was designed as a learning or adaptive flter. The adaptive filter has been the focus of several research proposals for new CMAC. In this work, we use a layer and neurobiological linkages approach, drawing inspiration from the Granule layer, the Molecular layer, and the Purkinje layer [23, 24] to design a controller for the cerebellum. It is often accepted that the granule layer serves as the input, the molecular layer as the learning, and the Purkinje layer as the output. Input signal activates the granule cells in the Cerebellum, where Mossy fibres from numerous axons enter. Cerebellar granule cells, which make up around three-quarters of all brain neurons, get input from mossy fner and use nerve cell parallel fber to stimulate Purkinje cells. Learning component Climbing fber will provide Purkinje cell the boost it needs. The Purkinje cell is the Cerebellum's final product.

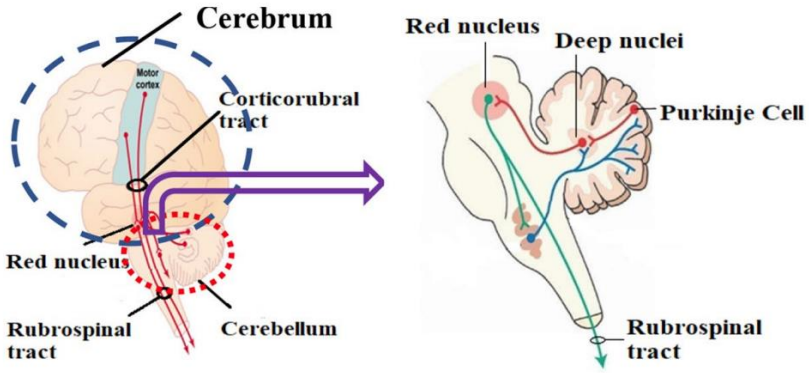

(a) Connectivity between Cerebrum and Red nucleus **(b) Connectivity between Cerebellum with Deep and Red nucleus**

Figure6. Integration of many brain modules in mammals

Inspiring neurobiological links between the brain's Cerebrum and Cerebellum allowed the authors of this article to create a multi-modular joint- Brain Controller (MMJ-BC). The Red Nucleus (RN) is a significant element located in the Midbrain of the Brainstem, which is responsible for motor coordination and execution in mammals by processing data from the Cerebrum and Cerebellum. Connections between the brain's Cerebrum and its RN are shown in Figure 1a. The RN is directly connected to the cerebellar motor cortex via the cortico-rubral track. The connections between the Cerebellum and RN are shown in Figure 1b. It has been discovered that a component of the Deep Nucleus (DN) called the Interpositus Nucleus is responsible for the communication between the Cerebellar cortex and the RN. The DN gets input from Purkinje cells and acts as the cerebellum's last integrator. In this study, we simply focus on the DN to keep things simple. DN links the cerebellar cortex to the RN by way of the cerebello-rubral tract (CRT). The spinal cord receives the processed data from the RN via the Rubro-Spinal Track (RST) [27]. The RST and spinal cord are modelled as a plant/nonlinear system on the surface of the MMJ-BC computational model. The development of MMJ-BC, however, requires a link to be made between the cerebrum and the RN, and the cerebellum and the DN, both of which are regarded to be part of the brain stem.

Mathematical modelling of MMJ-BC

Using mathematical relations, the neurobiological behaviour of the Cerebrum and Cerebellum with RN and DN connections may be modelled as MMJBC. Figure 2 depicts an MMJ-BC plant. To accomplish the reference/anticipated signal, the Cerebrum and Cerebellum analyse the Error signal (e) and output a control signal. The controller model incorporates links to the RELBIC and cerebellar reticular formation (RST and CRT). The RN provides the output for the MMJ-BC, with both controllers having their gains adjusted such that they provide the same result. Using a continuous approach, we find a number of different mathematical models for MMJ-BC, and we arrive at the following relations.

$$RN = y_{mmj} = f(y_{dn}, y_{bec}) \quad (31)$$

$$y_{mmj} = y_{dn} - y_{bec} \quad (32)$$

The Deep nucleus (DN) receives its information from the cerebellar cortex's output, namely the Purkinje cells' (PCs') and Climbing fibres' (CFs') projections.

$$y_{dn} = N.y_{ceb} = N.(P_c) = N.C_f.P_f \quad (33)$$

where N is a constant that may be determined by trial and error to be the desired weight. The amygdala and orbitofrontal cortex (OFC) are responsible for the BELBIC response, which may be represented as

$$y_{bec} = A_i - O_i \quad (34)$$

B. Mathematical modelling of BELBIC [10]

The amygdala and orbitofrontal cortex (OFC) system are combined to replicate the limbic system of the mammalian brain, which is responsible for emotional intelligence. The BELBIC approach is an automated system for generating actions in response to sensory data and motivational prompts. Depending on the task at hand, control engineering judgement guides the selection of sensory input, while the performance goals of the task dictate which emotional signals should be used.

The controller output (ybec) in the BELBIC method is determined by the sum of the excitations (controlled by the Amygdala) and the inhibitions (produced by the OFC) in Eq. (3).

$$A_i = S_i V_i \quad (35)$$

$$O_i = S_i W_i \quad (36)$$

Calculating shifts in Vi and Wi according to the associative learning rule requires only:

$$\Delta V_i = \alpha(S_{imax}(0, Rew - \sum_i A_i)) \quad (37)$$

$$\Delta W_i = \beta\big(S_i(E' - Rew)\big) \quad (38)$$

where a and b represent the amygdala's and OFC's respective stages of learning, and w represents the worth of an emotional signal (Reward). The dynamical system's BELBIC controller arrangement is shown in Figure 2. We have settled on the following sensory input and Reward function:

$$S_i = B_{1e} + B_2 \int e dt \quad (39)$$

$$Rew = B_{3e} + B_4 \int y_p dt + B_5 \frac{dy_p}{dt} \quad (40)$$

IX. where e is the deviation from the reference input signal, and yp is the output from the plant.

X. SIMULATION RESULTS AND DISCUSSION

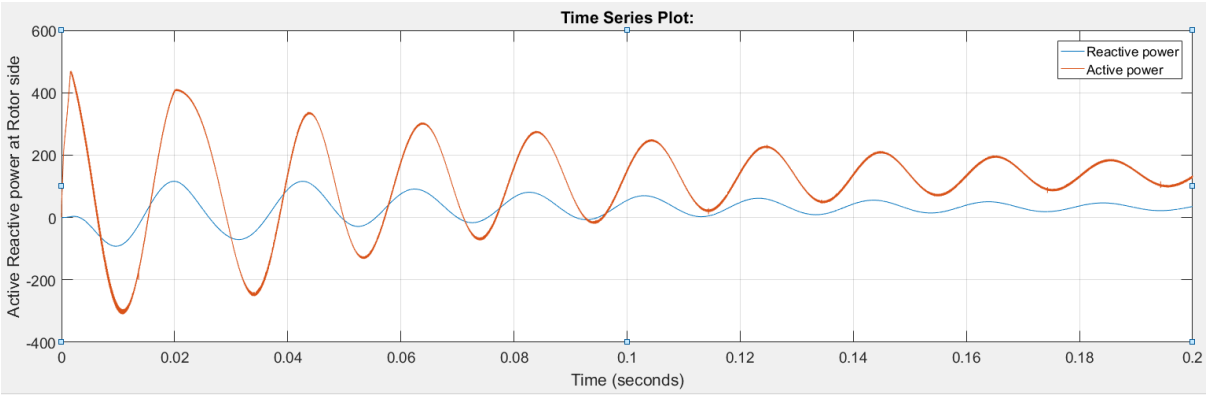

Figure 7. The DFIG rotor's active reactive power

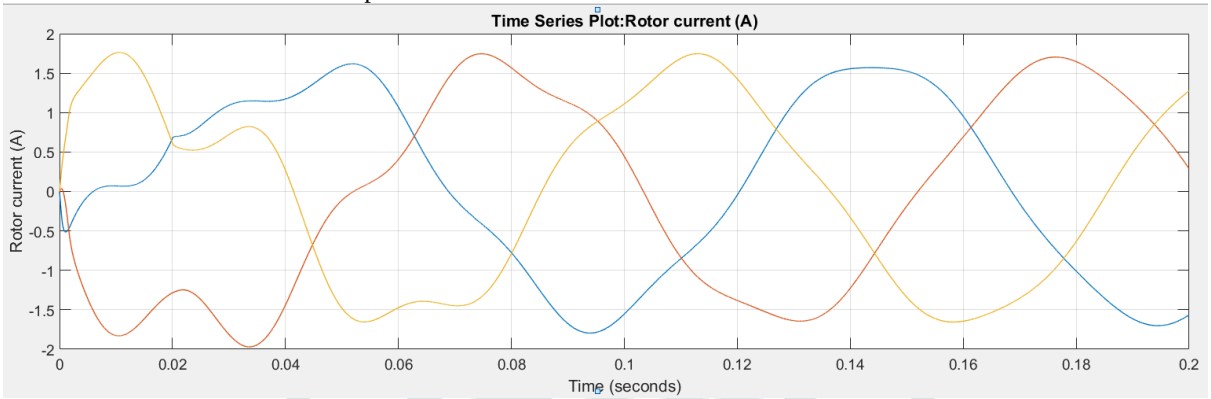

Figure8. The DFIG Rotor Currents

Figure 9. Power on the Grid, both active and reactive.

with this article, we examine RSC efficiency with a constant wind speed of 12 m/s. Fig.14 displays the transition from sub-synchronous to super-synchronous operation of the rotor side voltage and current using numerical values for all three phase voltage, current, power, and the power factor. All stator and rotor variables are DC in dq frame, allowing for easy, decoupled control. The 180-degree phase shift between the stator voltage and currents indicates that WECS is operating in the producing mode. As can be seen in Fig.8, the voltage and current at the grid terminal are in phase with one another. It exemplifies the power factor of unity. At 1200 rpm in sub-synchronous mode and 1500 rpm in super-synchronous mode, electricity flows from the grid to the rotor terminal, respectively. The electricity flows in both directions, from the rotor to the grid.

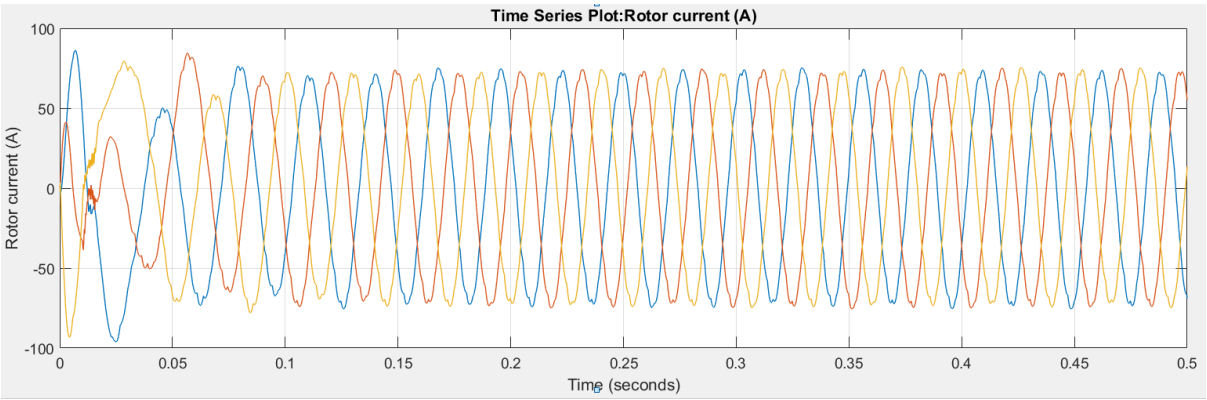

Figure10. The DFIG Rotor Currents

Current and voltage on the rotor side may be adjusted from subsynchronous to supersynchronous operation. All stator and rotor variables are DC in dq frame, allowing for easy, decoupled control. The 180-degree phase shift between the stator voltage and currents indicates that WECS is operating in the producing mode. As can be seen in Fig.10, the voltage and current at the grid terminals are in phase with one another. It exemplifies the power factor of unity.

Figure 11. Rapidity of the DFIG

At 1200 rpm rotor speed and a PI controller, electricity flows from the grid to the rotor terminal; at 1500 rpm rotor speed and a BELBIC, power flows in the other manner. The electricity flows in both directions, from the rotor to the grid.

CONCLUSION

Since the results show that the grid supply voltage, current, and frequency are in sync with the DFIG's produced output voltage, current, and frequency, we may infer that the Reactive power control of DFIG utilising FPGA module has been successfully implemented. Once DFIG has been synchronised with the Grid, it can be seen that active power control is acquired by adjusting the DC motor's speed or frequency, while reactive power control is attained by adjusting the generator's excitation voltage. Particularly in the case of islanded mode of micro grid operation, wind power production plays a significant role and provides a reasonable proportion to overall power generation of country. To connect an alternator to the grid, grid synchronisation will become more important. Using an FPGA increases its adaptability, and the code already present in the chip may be repurposed. Since reactive power may cause components to overheat, which drastically reduces the lifespan of machinery. Power factor regulation is another service that may be provided by DFIG via management of the reactive power exchange with the grid. Therefore, it maximises the use of technological devices and reduces expenses.

REFERENCES:

[1] S. Bull, “Renewable Energy today and tomorrow” Proc. IEEE, vol. 89, no. 8, pp. 1216- 1226, Aug. 2001.

[2] 20% Wind Energy By 2030: Increasing Wind Energy’s Contribution to U.S. Electricity Supply, U.S. Department ofEnergy, Jul. 2008.

[3] A. Barin, L. F. Pozzatti, L. N. Canha, R. Q. Machado, A. R. Abaide, and G. Arend, “Electrical power and energy systems multi-objective analysis of impacts of distributed generation placement on the operational characteristics.

[4] W. Qiao and R. G. Harley, “Grid connection requirements and solutions for DFIG wind turbines,” in Proc. IEEE EnergyConf., Atlanta, GA, Nov. 17–18, 2008, pp. 1–8.

[5] R. Piwko, D. Osborn, R. Gramlich, G. Jordan, D. Hawkins, and K. Porter, “Wind energy delivery issues: Transmission planning and competitive electricity market operation,” IEEE Power EnergyMag., vol. 3, no. 6, pp. 47–56, Nov./Dec. 2005.

[6] F. Blaabjerg, R. Teodorescu, M. Liserre, and A. V. Timbus, “Overview of control and grid synchronization for distributed power generation systems,”IEEE Trans. Ind. Electron., vol.53, no.4, pp.1398–1409, Oct.2006.